Low-voltage organic transistors based on solution processed semiconductors and self-assembled monolayer gate dielectrics

Woebkenberg, Paul H.; Ball, James; Kooistra, Floris B.; Hummelen, Jan C.; de Leeuw, Dago M.; Bradley, Donal D. C.; Anthopoulos, Thomas D.

Published in:
Applied Physics Letters

DOI:
10.1063/1.2954015

Publication date:
2008

Low-voltage organic transistors based on solution processed semiconductors and self-assembled monolayer gate dielectrics

Paul H. Wöbkenberg,[1] James Ball,[1] Floris B. Kooistra,[2] Jan C. Hummelen,[2] Dago M. de Leeuw,[3] Donal D. C. Bradley,[1] and Thomas D. Anthopoulos[1,a)]
[1]*Department of Physics, Blackett Laboratory, Imperial College London, London SW7 2BW, United Kingdom*
[2]*Molecular Electronics, Zernike Institute for Advanced Materials and Stratingh Institute of Chemistry University of Groningen, Nijenborgh 4, 9747 AG Groningen, The Netherlands*
[3]*Philips High-Tech Campus, Prof. Holstlaan 4, 5656 AA Eindhoven, The Netherlands*

(Received 28 May 2008; accepted 10 June 2008; published online 8 July 2008)

Reduction in the operating voltage of organic transistors is of high importance for successful implementation in low-power electronic applications. Here we report on low-voltage *n*-channel transistors fabricated employing a combination of soluble organic semiconductors and a self-assembled gate dielectric. The high geometric capacitance of the nanodielectric allows transistor operation below 2 V. Solution processing is enabled by analysis of the surface energy compatibility of the dielectric and semiconductor solutions. Electron mobilities in the range of $0.01-0.04\ \mathrm{cm^2/V\,s}$ and threshold voltages $\leqslant 0.35$ V are demonstrated. The present work paves the way toward solution processable low-voltage/power, organic complementary circuits. © *2008 American Institute of Physics*. [DOI: 10.1063/1.2954015]

Advances in solution processable organic field-effect transistors (OFETs) are sought for the realization of high throughput yet low-cost electronic applications. Examples include organic integrated circuits[1] for flexible displays[2] and radio-frequency identification tags.[3] Unfortunately, the vast majority of reported OFETs incorporating polymeric or inorganic gate insulators require high operating voltages. Paramount to the successful implementation of OFET technology in future device applications will be low-voltage operation.[4] A number of efforts have achieved this target but typically at the cost of solution processability of the semiconductor/gate dielectric.[4–13] The primary advantage associated with solution processing is the simple fabrication and potentially lower manufacturing cost. However, controlling the morphology of solution processed films is usually complex and performance optimization is determined by many interrelated parameters, particularly wetting behavior of the semiconductor solution on the surface of the dielectric or substrate.

The best results on low-voltage OFETs reported in literature come from devices employing self-assembled monolayer (SAM) gate dielectrics.[8–14] Collet *et al.*, for example, used carboxyl terminated tetradecylenyltrichlorosilane SAMs on Si wafers for the fabrication of OFETs using evaporated α-sexithiophene.[11] Transistor operation at <2 V was demonstrated with gate leakage currents of $\sim 10^{-6}\ \mathrm{A/cm^2}$. Other examples include work by Klauk *et al.*[10,12] where they demonstrated low-voltage OFETs based on octadecylphosphonic acid (ODPA) SAMs as the gate dielectric employing evaporated organic semiconductors. More recently, Ma *et al.* reported the use of alkylphosphonic acid and anthrylalkylphosphonic acid SAMs also in combination with evaporated films of organic semiconductors.[13] Unfortunately, inherent to most SAM-type dielectrics terminated with methyl groups is a low surface energy dominated by dispersive, i.e., nonpolar, interactions. This severely limits the range of soluble organic semiconductors that can be used to form high quality semiconducting films by spin coating. As a consequence, reports on low-voltage OFETs based on SAM dielectrics and solution processable organic semiconductors are scarce.[14]

Here we report on low-voltage organic transistors fabricated by spin coating the semiconductor onto gate electrodes functionalized with SAM dielectrics. By studying and understanding the surface characteristics of the SAM dielectric, we are able to develop semiconducting molecules with compatible surface properties sufficient for film formation via spin coating. As the SAM and organic semiconductor molecules we employ ODPA and side chain fluorinated methanofullerenes or fulleropyrrolidines, respectively.[15] Transistors with electron mobilities in the range of $0.01-0.04\ \mathrm{cm^2/V\,s}$ and operating voltages down to few volts are demonstrated.

Bottom-gate, top-contact OFETs were fabricated on glass substrates. Aluminum gate electrodes 30 nm thick were thermally evaporated under vacuum employing shadow masks. The gate electrodes were subsequently oxidized in oxygen plasma and then submerged in a 1 mM solution of ODPA in ethanol for several hours. Substrates were sonicated in ethanol followed by thermal annealing. Presence of the ODPA on the gate electrode surfaces was confirmed using contact angle measurements. Finally, the organic semiconductor layers were spin coated from 10 mg/ml solutions in chlorobenzene, followed by the deposition of Al source (S) and drain (D) electrodes. Electrical characterization of the transistors was carried out in nitrogen.

Contact angle measurements were performed on $\mathrm{Al-AlO_x}$ surfaces before and after treatment with the SAM using a Krüss DSA100 drop shape analysis system. Fig. 1(a) displays images of a water droplet on the two surfaces. It is evident that upon treatment with ODPA [Fig. 1(b), inset] the contact angle (θ) changes from 40° to 110°, indicating the presence of ODPA. Metal-insulator-metal diode structures were fabricated for determining the leakage current and geometric capacitance (C_i) of the dielectric before and after treatment. Fig. 1(b) shows the current density-voltage (J-V) characteristics measured for three diodes fabricated employing Al electrodes that have been treated differently. A striking observation is the drastic reduction in the leakage current

a)Author to whom correspondence should be addressed. Electronic mail: thomas.anthopoulos@imperial.ac.uk.

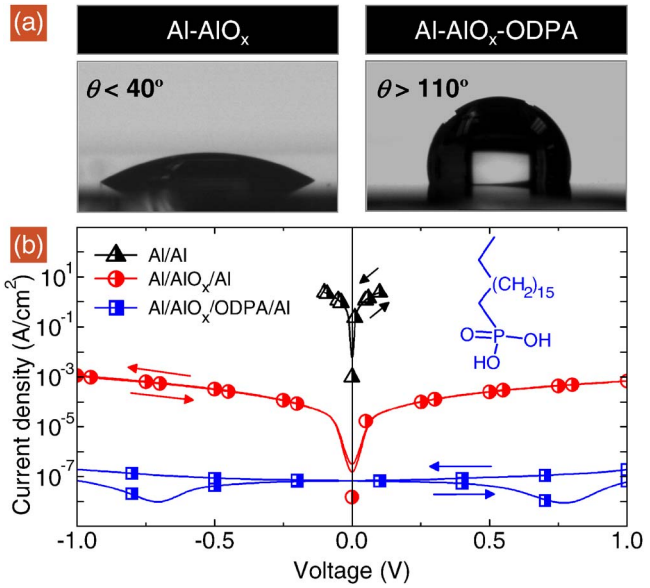

FIG. 1. (Color online) (a) Water droplets on Al–AlO$_x$ (left) and on Al–AlO$_x$-ODPA (right). (b) Current density vs bias voltage for diodes fabricated with untreated Al electrodes (triangles), oxidized bottom electrode (circles) and ODPA functionalised Al–AlO$_x$ bottom electrode (squares). Inset: molecular structure of ODPA.

upon treatment with ODPA. The measured geometric capacitance of the latter was in the range of 600–800 nF/cm^2.

Having established the suitability of ODPA SAMs as gate dielectrics, we attempted to fabricate OFETs employing a number of soluble organic molecules [Fig. 2(a)]. Unfortunately, wetting of the Al–AlO$_x$-ODPA surface by several different semiconductor solutions was found to be very problematic, with few exceptions. In order to study and understand the interplay between the surface properties of the dielectric and the semiconductor solutions we carried out a series of surface energy measurements. The dispersive and polar solid surface energy components of the SAM were calculated by measuring the contact angles of three different liquids (whose polar and dispersive components were known) on the solid surface. Following the Owens–Wendt–Kaelble method[16], solid surface energy components can be extracted from a linear fit to Eq. (1), derived from the Owens–Wendt–Kaelble and Young's equations,[16]

$$\frac{\gamma_L(\cos\theta+1)}{2(\gamma_L^D)^{1/2}} = (\gamma_S^P)^{1/2}\left(\frac{\gamma_L^P}{\gamma_L^D}\right)^{1/2} + (\gamma_S^D)^{1/2}. \quad (1)$$

Here, θ is the equilibrium contact angle made by each liquid on the solid surface and γ is the surface energy where superscripts D and P refer to the dispersive part and the polar part respectively. The subscripts L and S refer to the liquid and solid, respectively. Measurements of Al–AlO$_x$-ODPA yielded γ_S^P=0.24 mN/m and γ_S^D=22.9 mN/m. Similarly, γ_L^P and γ_L^D for the organic semiconductor solutions were calculated from contact angles of the solutions on two different solid surfaces (whose polar and dispersive components were known) using Eq. (2) also derived from the Owens–Wendt–Kaelble and Young's equations,

$$\gamma_L^D = \left\{\frac{\gamma_L(\cos\theta_1+1)(\gamma_{S2}^P)^{1/2} - \gamma_L(\cos\theta_2+1)(\gamma_{S1}^P)^{1/2}}{2[(\gamma_{S1}^D\gamma_{S2}^P)^{1/2} - (\gamma_{S2}^D\gamma_{S1}^P)^{1/2}]}\right\}^2. \quad (2)$$

Here, subscripts 1 and 2 refer to solids 1 and 2, respectively. The total surface energy of each liquid ($\gamma_L=\gamma_L^P+\gamma_L^D$) was measured from analysis of pendant drops of solutions. Caution is advised to experimenters following this method as it has been suggested that large differences between liquid and solid surface energy components used in these calculations can lead to significant experimental error.[16] To quantify the wettability of each solution on the SAM surface it is useful to compute the spreading parameter $\Delta W=\gamma_L(\cos\theta-1)$.[17] The latter represents the difference between the work of adhesion ($W_{SL}=\gamma_L(\cos\theta+1)$, i.e. the work required to separate a unit area of the solid-liquid interface) and the work of cohesion ($W_{LL}=2\gamma_L$, i.e. the work required to separate a unit area of liquid-liquid interface).[18] ΔW shows the extent to which the liquid will adhere to the surface relative to itself and hence indicates the ability of a liquid drop to stick to the solid surface during solution processing. At θ=0°, ΔW=0 indicating that the liquid can adhere equally well to the surface of the solid as it does to itself and hence complete wetting is observed.

Another useful illustration of the wetting behavior of liquids on the Al–AlO$_x$-ODPA surface can be gained from determining their wetting envelopes. These are lines of constant equilibrium contact angle on a plot of γ_L^P versus γ_L^D, determined by suitable manipulation of Eq. (1). The plot, shown in Fig. 2(b), gives an indication of the degree to which various liquids will wet the surface if γ_L^P and γ_L^D are known. It also illustrates the surface properties of ideal liquids for solution processing on the SAM. As is implicit from $\Delta W=\gamma_L(\cos\theta-1)$, smaller contact angles will generally be associated with increased wettability. Any liquids whose surface energy components plotted on the graph lie below the

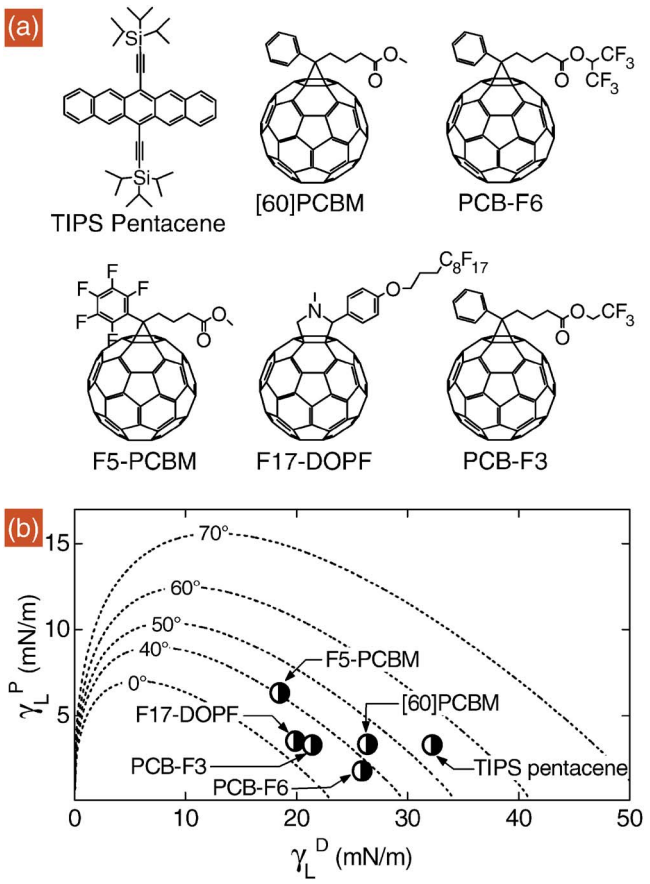

FIG. 2. (Color online) (a) Chemical structure of the molecules studied. (b) Wetting envelopes for the AlO$_x$-ODPA surface with coordinates of liquid surface energy components of semiconductor solutions plotted (symbols).

TABLE I. Summary of material properties and device characteristics. All measurements were performed using 10 mg/ml chlorobenzene solutions except triisopropylsilyl-pentacene (TIPS-pentacene) which was measured using a 40 mg/ml tetralin solution.

	Parameter							
Molecule	γP (mN/m)	γD (mN/m)	θ (°)	ΔW (mN/m)	μ ($cm^2/V\,s$)	V_T (V)	S (mV/decade)	I_{on}/I_{off}
F17-DOPF	3.5	19.9	25.0	−2.2	0.04	0.35	110	10^4
PCB-F3	3.3	21.4	33.3	−4.1	0.01	0.13	200	10^3
PCB-F6	1.8	25.9	37.5	−5.7	···	···	···	···
F5-PCBM	6.3	18.5	40.1	−5.8	···	···	···	···
[60]PCBM	3.4	26.4	42.8	−7.9	···	···	···	···
TIPS-pentacene	3.3	32.2	51.7	−13.5	···	···	···	···

line of $\theta=0°$ will completely wet the surface. Liquids whose surface energy components lie above the line of $\theta=40°$ do not demonstrate particularly good wetting and good film formation from solution processing becomes less likely. Hence, for use with ODPA, candidate semiconductor solutions should possess low surface energies dominated by dispersive rather than polar forces (i.e., $\gamma_L^P \sim 0$ and ideally $\gamma_L^D \leqslant \gamma_S^D$).

Figure 2(b) also displays plots of the coordinates of a number of organic semiconductor solutions. The experimentally determined contact angles and surface energy components for each material are summarized in Table I. We observe that those solutions with $\Delta W < -5$ mN/m and whose surface energy components lie to the right of the $\theta=40°$ wetting envelope did not demonstrate transistor operation. Upon spin coating, these solutions formed inhomogeneous films or no film at all. Interestingly, two solutions, F17-DOPF and PCB-F3 (10 mg/ml in chlorobenzene), are seen to approach the surface energy characteristics required for wetting the Al–AlO_x-ODPA surface. Upon spin coating, these solutions are found to form continuous films that are suitable for use in OFETs. To demonstrate this we fabricated transistors [see the inset in Fig. 3(b)] employing an ODPA SAM dielectric and F17-DOPF/PCB-F3 as the semiconductors. The transistor parameters calculated are summarized in Table I. Figure 3 displays the transfer [drain current (I_D) versus gate voltage (V_G) [Fig. 3(a)]] and output (I_D versus drain voltage (V_D) at different V_G [Fig. 3(b)]) characteristics of a F17-DOPF OFET. Electron mobility in the range of 0.01–0.04 $cm^2/V\,s$ and threshold voltages of $\leqslant$0.35 V [Fig. 3(a)] are calculated. The current on/off ratio and subthreshold slope ($S = \partial V_G / \partial \log_{10} I_D$) were also estimated yielding $\sim 10^4$ and $\sim$110 mV/decade, respectively.

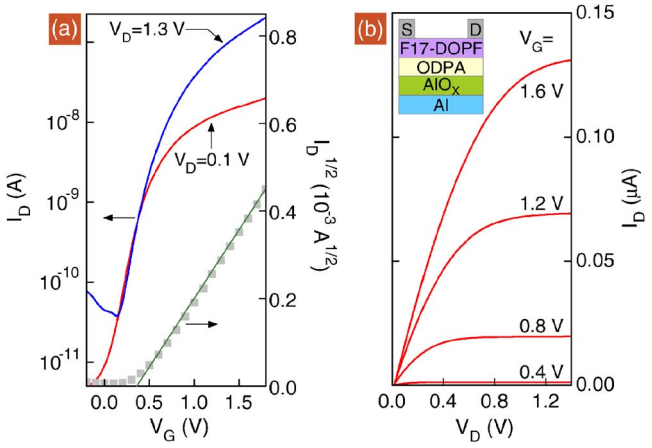

FIG. 3. (Color online) Transfer (a) and output (b) curves for a representative F17-DOPF based OFET with channel length and width of 60 μm, and 1 mm, respectively. Inset: schematic of the OFET architecture employed.

In summary, by studying and understanding the surface energy interactions between the AlO_x-ODPA dielectric and a number of soluble organic semiconductors we were able to demonstrate SAM enabled low-voltage *n*-channel OFETs fabricated from solution. Our method of surface analysis to determine the suitability of soluble organic semiconductors for processing on a given solid surface is generic and should be applicable to a wide range of SAM dielectric/organic semiconductor systems. This work could have significant implications for the development of low-voltage, low-power solution processed organic circuits.

The authors are grateful to P. Hotchkiss and S. Marder from Georgia Institute of Technology for insightful discussions on SAM functionalisation.

[1] B. Crone, A. Dodabalapur, Y.-Y. Lin, R. W. Filas, Z. Bao, A. LaDuca, R. Sarpeshkar, H. E. Katz, and W. Li, Nature (London) **403**, 521 (2000).
[2] L. Zhou, A. Wanga, S.-C. Wu, J. Sun, S. Park, and T. N. Jackson, Appl. Phys. Lett. **87**, 083502 (2006).
[3] P. F. Baude, D. A. Ender, M. A. Haase, T. W. Kelley, D. V. Muyres, and S. D. Theiss, Appl. Phys. Lett. **82**, 3964 (2003).
[4] A. Facchetti, M.-H. Yoon, and T. J. Marks, Adv. Mater. (Weinheim, Ger.) **17**, 1705 (2005).
[5] C. D. Dimitrakopoulos, I. Kymissis, S. Purushothaman, D. A. Neumayer, P. R. Duncombe, and R. B. Laibowitz, Adv. Mater. (Weinheim, Ger.) **11**, 1372 (1999).
[6] M. J. Panzar, C. R. Newman, and C. D. Frisbie, Appl. Phys. Lett. **86**, 103503 (2005).
[7] S. H. Kim, S. Y. Yang, K. Shin, H. Jeon, J. W. Lee, K. P. Hong, and C. E. Park, Appl. Phys. Lett. **89**, 183516 (2006).
[8] M. Halik, H. Klauk, U. Zschieschang, G. Schmid, C. Dehm, M. Schütz, S. Maisch, F. Effenberger, M. Brunnbauer, and F. Stellacci, Nature (London) **431**, 963 (2004).
[9] M.-H. Yoon, A. Facchetti, and T. J. Marks, Proc. Natl. Acad. Sci. U.S.A. **102**, 4678 (2002).
[10] H. Klauk, U. Zschieschang, J. Pflaum, and M. Halik, Nature (London) **445**, 745 (2007).
[11] J. Collet, O. Tharaud, A. Chapoton, and D. Vuillaume, Appl. Phys. Lett. **76**, 1941 (2000).
[12] H. Klauk, U. Zschieschang, and M. Halik, J. Appl. Phys. **102**, 074514 (2007).
[13] H. Ma, O. Acton, G. Ting, J. W. Ka, H.-L. Yip, N. Tucker, R. Schofield, and A. K.-Y. Jen, Appl. Phys. Lett. **92**, 113303 (2008).
[14] Y. D. Park, D. H. Kim, Y. Jang, M. Hwang, J. A. Lim, and K. Cho, Appl. Phys. Lett. **87**, 243509 (2005).
[15] P. H. Wöbkenberg, J. Ball, D. D. C. Bradley, T. D. Anthopoulos, F. Kooistra, J. C. Hummelen, and D. M. de Leeuw, Appl. Phys. Lett. **92**, 143310 (2008).
[16] D. Y. Kwok and A. W. Neumann, Adv. Colloid Interface Sci. **81**, 167 (1999).
[17] P. G. de Gennes, Rev. Mod. Phys. **57**, 827 (1985).
[18] J. Zhang and D. Y. Kwok, J. Phys. Chem. B **106**, 12594 (2002).